Activity profiling of SARS-CoV-2-PLpro protease provides structural framework for anti-COVID-19 drug design

Wioletta Rut[1*], Mikolaj Zmudzinski[1], Zongyang Lyu[2,5], Digant Nayak[2,5] Scott J. Snipas[3], Miklos Bekes[4,6], Tony T. Huang[4], Shaun K. Olsen[2,5*], Marcin Drag[1,3*]

[1]Department of Chemical Biology and Bioimaging, Wroclaw University of Science and Technology, Wyb. Wyspianskiego 27, 50-370 Wroclaw, Poland

[2] Department of Biochemistry & Molecular Biology and Hollings Cancer Center, Medical University of South Carolina, Charleston, SC, 29425, USA

[3]Sanford Burnham Prebys Medical Discovery Institute, 10901 North Torrey Pines Road, La Jolla, CA 92037, USA

[4]Department of Biochemistry & Molecular Pharmacology, New York University School of Medicine, New York, NY 10016, USA

[5]present address: Department of Biochemistry & Structural Biology University of Texas Health Science Center at San Antonio, San Antonio, TX, 78229 USA

[6]present address: Arvinas, Inc., 5 Science Park, New Haven, CT, 06511, USA

Corresponding authors: wioletta.rut@pwr.edu.pl, olsens@uthscsa.edu, marcin.drag@pwr.edu.pl

Abstract

In December 2019, the first cases of a novel coronavirus infection causing COVID-19 were diagnosed in Wuhan, China. Viral Papain-Like cysteine protease (PLpro, NSP3) is essential for SARS-CoV-2 replication and represents a promising target for the development of antiviral drugs which would be facilitated by an understanding of its substrate specificity. Here, we used a combinatorial substrate library containing natural and a wide variety of nonproteinogenic amino acids and performed comprehensive activity profiling of SARS-CoV-2-PLpro. We found that the P2 site of SARS-CoV-2-PLpro is highly specific for Gly, the P3 site exhibits a high degree of promiscuity, and the P4 site exhibits a preference for amino acids with hydrophobic side chains. We also demonstrate that SARS-CoV-2-PLpro harbors deubiquitinating activity. Both the substrate binding profile and deubiquitinating activity are shared with the highly related SARS-CoV-PLpro which harbors near identical S4-S2 binding pockets. On the scaffold of best hits from positional scanning we have designed optimal fluorogenic substrates and irreversible inhibitors with a high degree of selectivity for SARS PLpro variants versus other proteases. Altogether this work has revealed the molecular rules governing PLpro substrate specificity and provides a framework for development of inhibitors with potential therapeutic value or drug repositioning.

Keywords: papain like protease, COVID-19, coronavirus, cysteine protease

Introduction

The global epidemic of three coronaviruses have emerged in this century so far. In November 2002 in Foshan, China, the first known case of human infected with severe acute respiratory syndrome coronavirus (SARS-CoV) has been reported [1]. By July 2003, more than 8,000 SARS cases were detected in 27 countries. The main symptoms of SARS-CoV infection were influenza-like and included fever, headache, malaise, shivering and diarrhea. Only a few cases of infection occurred between December 2003 and January 2004 [2]. The implementation of measures infection control has ended the global SARS outbreak. Ten years after the SARS pandemic a new coronavirus – Middle East respiratory syndrome coronavirus (MERS-CoV) was diagnosed in Saudi Arabia man [3]. Due to international travels of infected people, MERS-CoV has spread worldwide. 2502 laboratory-confirmed cases of MERS-CoV infection were reported from September 2012 to the end of December 2019, including 858 associated deaths. In December 2019 a novel coronavirus - severe acute respiratory syndrome coronavirus 2 (SARS-CoV-2) formerly known as the 2019 novel coronavirus (2019-nCoV) was identified in Wuhan, China [4, 5]. Current studies indicate that this coronavirus is similar to SARS-CoV. Although these three coronaviruses - SARS-CoV, MERS-CoV, and SARS-CoV-2 are identified as a highly pathogenic into the human population, there is no effective antiviral treatment. Therefore, current studies are focused on rapid development of vaccines and antiviral drugs to prevent and treat coronavirus infection.

One of the attractive antiviral drug targets is the SARS-CoV encoded cysteine protease – papain-like protease (PLpro) [6]. This enzyme recognizes the tetrapeptide LXGG motif found in-between viral proteins nsp1 and nsp2, nsp2 and nsp3, and nsp3 and nsp4 (nsp1/2, nsp2/3, nsp3/4) [7, 8]. The hydrolysis of the peptide bond on the carboxyl side of glycine at the P1 position leads to the release of nsp1, nsp2, and nsp3 proteins, which are essential for viral replication. The *in vitro* studies have shown that SARS-CoV-PLpro harbors two other proteolytic activities, removal of ubiquitin (Ub) and ubiquitin-like protein ISG15 (interferon-induced gene 15) from cellular proteins [9-11]. Ubiquitinated and ISGylated substrates are more efficiently hydrolyzed by SARS-CoV-PLpro than small substrates containing C-terminal LRGG motif [11, 12]. These results indicated a more complex mechanism of substrate recognition than only the interaction of S4-S1 pockets of enzyme with tetrapeptide fragment. Further studies revealed that SARS-CoV-PLpro possess two distinct Ub binding subsites (SUb1 and SUb2) and recognize Lys48-linked polyUb chains for polyubiquitin chain editing and/or deubiquitination of polyubiquitinated proteins [13-15].

Due to the deubiquitinating and deISGylating activities of SARS-CoV PLpro, this enzyme performs significant role in the innate immune response during viral infection [16, 17]. SARS-CoV-PLpro is involved in inhibiting the production of cytokines and chemokines, that are responsible for the activation of the host innate immune response against viral infection [18-20]. For these reasons, this enzyme is an important molecular target in the design of SARS-CoV antiviral drugs. Despite substantial research efforts in the development of SARS-CoV inhibitors, efficacy data of these compounds from clinical trials are missing [21-23]. Nevertheless, we hypothesize that information gained over past years for the SARS-CoV-PLpro could be immediately translated into the timely study of SARS-CoV-2-PLpro to accelerate new antivirals development and drug retargeting approaches. The optimal method to check level of similarity in binding site architecture between two enzymes is positional scanning technology. We have developed recently a novel chemical approach, called HyCoSuL (Hybrid Combinatorial Substrate Library), to dissect a broad substrate specificity of proteolytic enzymes [24]. The use of natural and a wide range of unnatural amino acids in HyCoSuL structure allows for ultrafast discovery of highly active and selective substrates, inhibitors, and activity-based probes for multiple proteases. Using this approach leads to tens of millions of possible amino acid sequence combinations that can be measured revealing fingerprints of investigated enzymes, making it ideal for application in this current study.

Results

Substrate specificity profile

Our previous studies of SARS-CoV-PLpro substrate preferences using a combinatorial substrate library containing only natural amino acids revealed that this protease recognizes LXGG motif at P4-P1 positions with broad substrate specificity at P3 position [25]. These results suggest that more detailed mapping of binding pocket architecture should facilitate design of new, active substrates as well as optimal peptide sequences for inhibitor development efforts. To achieve this goal we developed a defined and combinatorial substrate library (HyCoSuL) containing wide variety of nonproteinogenic amino acids [24]. Since tetrapeptide fluorogenic substrates are not very efficiently hydrolyzed by enzymes exhibiting deubiquitinating activity, we designed and synthesized the P2 defined library with a general structure of Ac-LRXG-ACC (X – 19 natural and 109 unnatural amino acids) and a hybrid combinatorial substrate library, where three positions were fixed and one position contains an equimolar mixture of 19 amino acids (Mix), (P3 sublibrary: Ac-Mix-P3-Gly-Gly-ACC, P4 sublibrary: Ac-P4-Mix-Gly-Gly-ACC; P3 and P4 – a natural or unnatural amino acid) [26]. By

design of libraries with tailored peptide scaffold toward DUBs we could reach the highest possible concentration of individual fluorogenic substrates in each sublibrary during the assay. P2 library screening revealed that SARS-CoV and SARS-CoV-2-PLpro possess very high substrate specificity at this position – only glycine can be accepted (Figure 1). Both proteases exhibit a broad substrate preference at P3 position. The S3 pocket of SARS-CoV and SARS-CoV-2-PLpro can tolerate not only positively charged residues like Phe(guan), Dap, Dab, Arg, Lys, Orn, and hArg, but also hydrophobic amino acids, such as hTyr, Phe(F5), Cha, Met, Met(O), Met(O)$_2$, D-hPhe (amino acid structures presented in Table S1 supplemental information). These enzymes do not recognize acidic residues and most of D-amino acids (the exception are D-Arg, D-hPhe, D-Lys, and D-Phg). The S4 pocket of SARS-CoV and SARS-CoV-2-PLpro can accommodate hydrophobic residues only, among natural amino acids, practically only leucine can be tolerated (being the best hit for SARS-CoV-2-PLpro) (Figure 1). SARS-CoV-PLpro recognized two unnatural residues better than leucine at P4 position (hTyr and hTyr(Me)). Other bulky amino acids are also accepted (≥ 30%, hPhe, Abu(Bth), Phe(3-I), Cys(Bzl), Cys(MeBzl), Cys(4-MeOBzl), hSer(Bzl), and Dht).

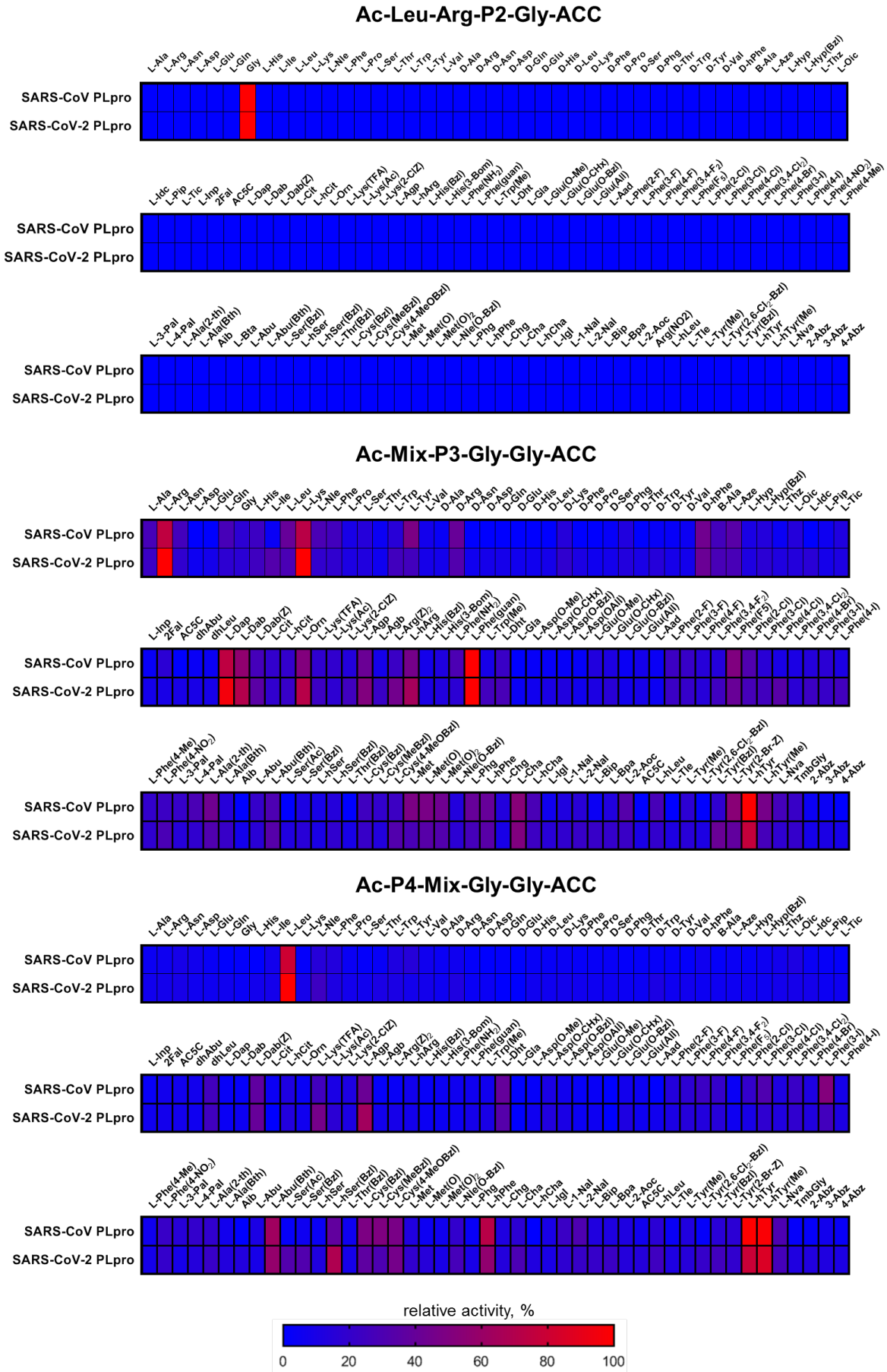

Figure 1. SARS-CoV-PLpro and SARS-CoV-2-PLpro substrate specificity profiles presented as heat maps.

Design and kinetic analysis of tetrapeptide fluorogenic substrates

To validate the library-screening data we designed optimal tetrapeptide fluorogenic substrates to find optimal sequences recognized by SARS-CoV and SARS-CoV-2-PLpro. We analyzed both SARS PLpro substrate specificity profile at the P4-P2 positions and selected the most preferred amino acids (P2: Gly; P3: Dap, Phe(guan); P4: hTyr, hPhe, and Abu(Bth)). Kinetic analysis revealed that some designed substrates were better recognized by SARS-CoV-PLpro with Ac-hTyr-Dap-Gly-Gly-ACC being almost 2.5 times more efficiently cleaved than endogenous Ac-LRGG-ACC.

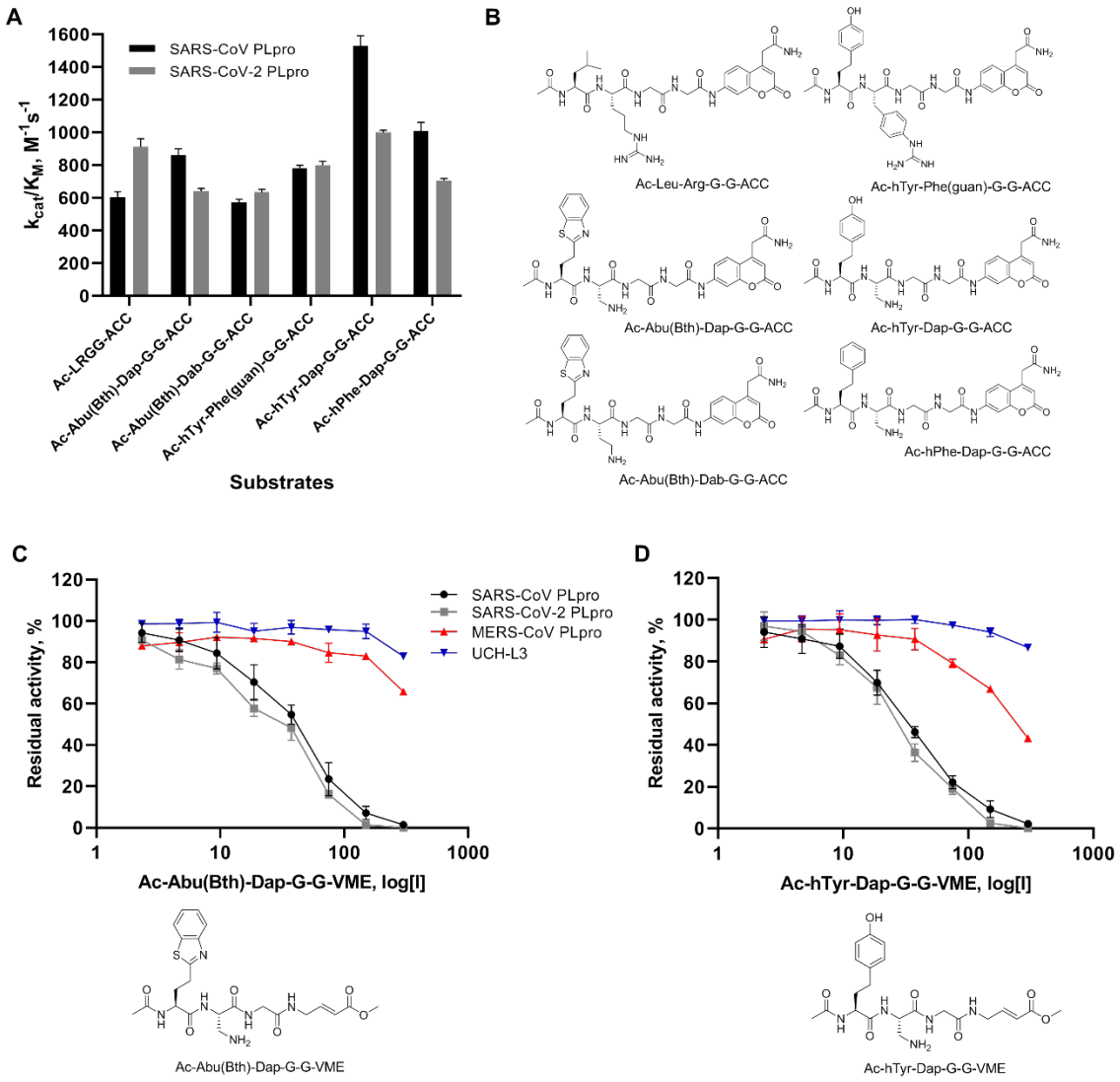

Figure 2. SARS-CoV-PLpro and SARS-CoV-2-PLpro substrate and inhibitor selectivity. (A) k_{cat}/K_M for tetrapeptide fluorogenic substrates toward SARS-CoV-PLpro and SARS-CoV-2 PLpro. (B) Tetrapeptide substrate structures. (C, D) DUBs inhibition by designed inhibitors ([I]=2.3-300 μM; SARS-CoV-PLpro concentration, 0.3 μM; SARS-CoV-2-PLpro concentration, 0.1 μM; MERS-CoV PLpro concentration, 2.5 μM; UCH-L3 concentration, 8 μM).

In case of SARS-CoV-2-PLpro, we did not find significant difference between Ac-LRGG-ACC and all tested substrates (Figure 2A). It is important to notice that substitution of Arg in P3 position by relatively small Dap did not affect binding to S3 pocket and yields very good substrates. Thus, data obtained from combinatorial screening very well translate into individual substrates and demonstrate very high level of similarity between two investigated enzymes.

Next, we wanted to see if incorporation of unnatural amino acids in P4 and P3 positions of peptide sequence can result in selective tetrapeptide substrates. We tested the substrates with four enzymes that exhibit deubiquitinating activity – SARS-CoV-PLpro, SARS-CoV-2-PLpro, MERS-CoV-PLpro and human DUB UCH-L3. We have found that none of the substrates with unnatural amino acids in the sequence were significantly recognized at 10μM either by MERS-CoV-2 PLpro (2.5 μM) nor human DUB UCH-L3 (8 μM). In line with previous data, Ac-LRGG-ACC was recognized by all four enzymes (Figure 3).

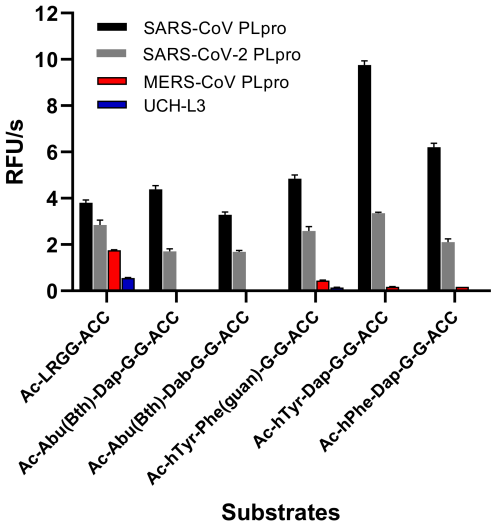

Figure 3. The rate of tetrapeptide substrate hydrolysis by DUBs. ([S]=10 μM; SARS-CoV PLpro concentration, 0.2 μM; SARS-CoV-2 PLpro concentrations, 0.1 μM; MERS-CoV PLpro concentration, 2.5 μM; UCH-L3 concentration, 8.8 μM).

Development of PLpro inhibitors

To further analyze selectivity of peptide sequences with unnatural amino acids we converted two substrates (Ac-hTyr-Dap-Gly-Gly-ACC and Ac-Abu(Bth)-Dap-Gly-Gly-ACC) into inhibitors by exchanging the fluorescent tag to a reactive group – vinylmethyl ester (VME). VME group was selected due to its broad reactivity toward DUBs (inhibitor selectivity is

determined by tetrapeptide sequence). The results from kinetic analysis of SARS-CoV-PLpro and SARS-CoV-2-PLpro inhibitors reflected those of substrate hydrolysis (Figure 2C, D). Ac-hTyr-Dap-Gly-Gly-VME was more potent but less selective inhibitor toward these enzymes than Ac-Abu(Bth)-Dap-Gly-Gly-VME. Importantly, both compounds exhibit high selectivity for SARS-PLpro variants and robustly inhibit both SARS-CoV-PLpro, SARS-CoV-2-PLpro activities. In contrast, practically no inhibition of human UCH-L3 and only a slight inhibition of MERS-PLpro was observed (Figure 2C, D). This is an important finding in search for selective antiviral molecule with minimal cross-reactivity with human DUBs.

SARS-CoV-2-PLpro recognizes ubiquitin protein

Studies carried out for SARS-CoV-PLpro revealed that this enzyme has ubiquitin binding domain and efficiently process full ubiquitin fluorogenic substrate [12]. We wanted to see if this is also the case for SARS-CoV-2-PLpro. Indeed, we found that the enzyme processes Ub-ACC substrate around 10 times more efficiently comparing to tetrapeptidic sequence Ac-LRGG-ACC (Table 1).

Enzyme	**k_{cat}/K_M, $M^{-1}s^{-1}$**	
	Ac-LRGG-ACC	**Ub-ACC**
SARS-CoV PLpro	601 ± 36	42 383 ± 1648
SARS-CoV-2 PLpro	912 ± 49	8 670 ± 417

Table 1. Kinetic parameters of selected substrates for SARS-CoV-PLpro and SARS-CoV-2-PLpro

Next, we used ubiquitin activity-based probe (ABP) for labelling of both enzymes. In this ABP biotin was used as detection tag and VME as irreversible warhead. To test its sensitivity, we performed SDS-PAGE analysis followed by nitrocellulose membrane transfer and visualization with fluorescent streptavidin (Figure 4). We observed significant labeling of both proteases by Biotin-Ub-VME at a concentration twice higher than the enzyme concentration (200 nM), however SARS-CoV-PLpro seem to be a little more efficiently labelled.

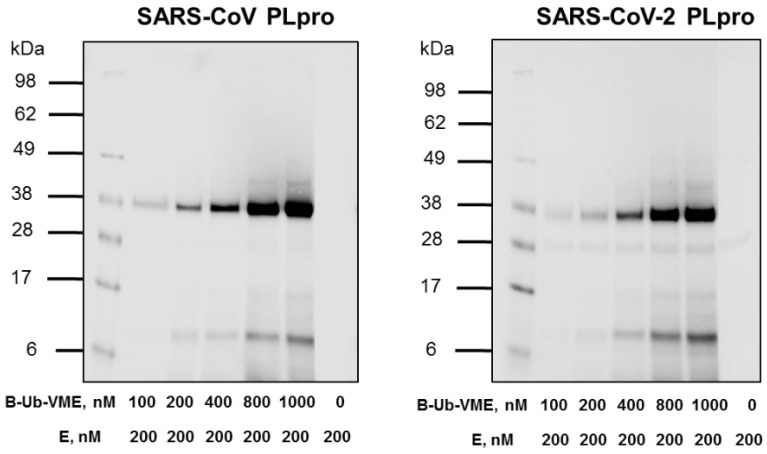

Figure 4. SARS-CoV-PLpro and SARS-CoV-2-PLpro labelling by Biotin-Ub-VME.

Discussion and Conclusions

The outbreak of the current coronavirus pandemic leading to COVID-19 disease has dramatically accelerated research into effective drugs and a vaccine to treat this disease. The genome of severe acute respiratory syndrome coronavirus 2 (SARS-CoV-2) consists of 29811 nucleotides that encode 29 proteins, two of which are proteases. The first of these, SARS-CoV-2-Mpro is used by the virus in the process of protein maturation. Its structure has already been described recently [27]. The results of retargeting about 12,000 drugs and other leading structures resulted in selection of several candidates for further studies [28]. To date, there is no information about the activity of the second protease, namely SARS-CoV-2-PLpro. We were hypothesizing that this enzyme, similarly to SARS-CoV-PLpro, in addition to participating in the process of virus protein maturation, also performs an additional function, which is to help the virus in evasion of the host innate immune responses by controlling the deubiquitination and deISGylation process. Thus, SARS-CoV-2-PLpro is also an excellent candidate for a drug, not only blocking virus replication, but also inhibiting the dysregulation of signaling cascades in infected cells [9]. Knowledge of substrate preferences is equally important with understanding the structure of the protein, as it enables rational design of inhibitors or research on drug retargeting.

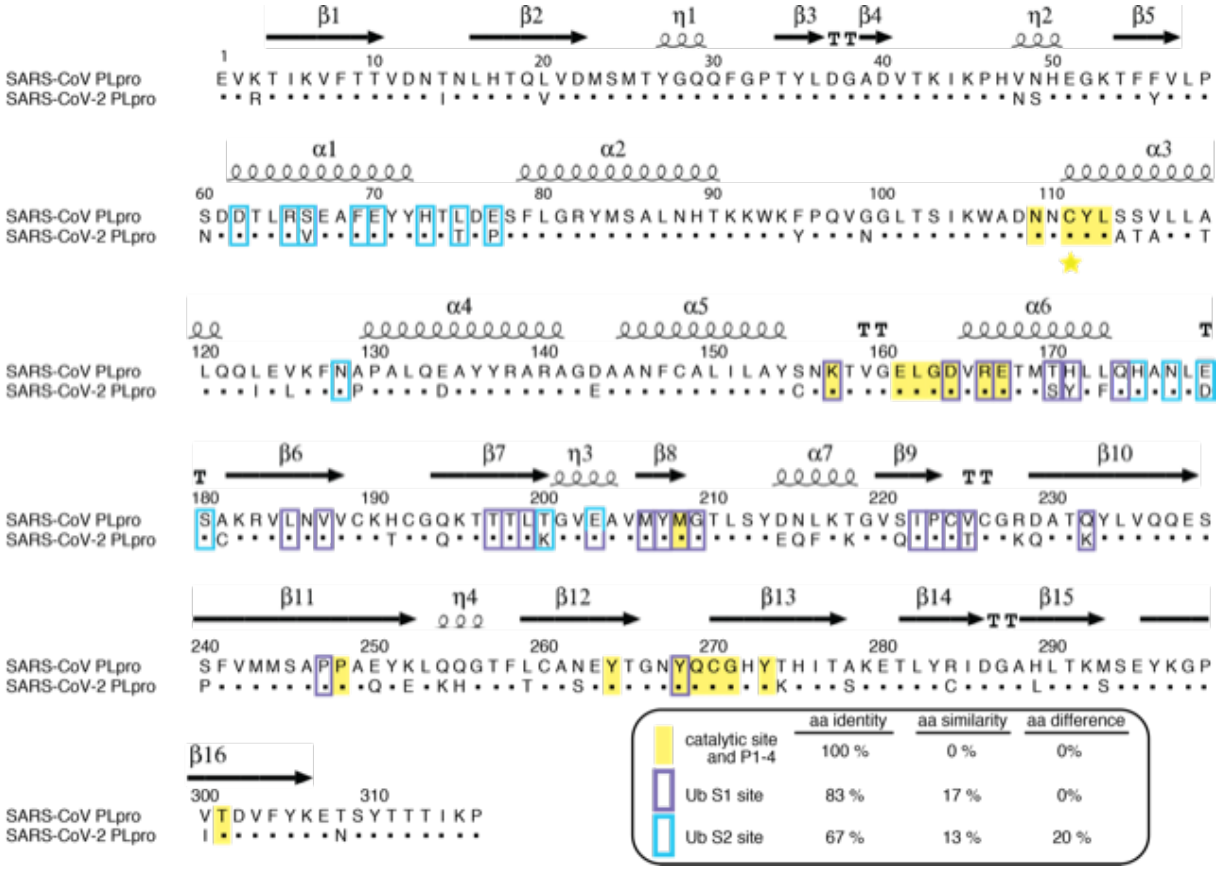

Figure 5. Sequence alignment of the PLpro from SARS and SARS2 (Covid19) were determined using default ClustalX parameters. Secondary structure was shown above sequence according to PDB 5E6J. Conserved residues are shown as dots. Catalytic cysteines were labeled with a yellow star. Residues involved in contacts with S1 Ubiquitin residue 73-76 are shaded yellow. Residues involved in contacts with S1 Ubiquitin residue 1-72 are boxed in purple line. Residues involved in contacts with S2 Ubiquitin are boxed in blue line.

In our research, we decided to examine the SARS-CoV-2-PLpro substrate preferences at positions P4-P2 and compare them directly with the well-known SARS virus 2002/03 protein, SARS-CoV-PLpro. For this purpose, we used positional scanning technology using natural and unnatural amino acids (HyCoSuL). Library screening revealed that both enzymes recognize only Gly in P2 and possess broad in P3 and rather narrow substrate specificity at the P4 position. Moreover, direct analysis of the preferences of both enzymes demonstrate that the architecture of S4-S2 pockets is almost identical, because they recognize natural and unnatural amino acids practically in a very similar way. The differences in activity for a given amino acid between the two enzymes observed in some positions are very small, and there are no amino acids that are recognized by one enzyme only. This is also confirmed by the analysis of amino acids building S4-S2 pockets in both enzymes, which is identical (Figure 5). This is critically important

information in the aspect of using information from research on inhibitors or retargeting of drugs conducted in the past for SARS-CoV-PLpro for immediate application to SARS-CoV-2-PLpro. Analysis of kinetic parameters for tetrapeptide substrates for both enzymes shows a high degree of similarity in terms of k_{cat}/K_m values, proving that the catalytic yields of both enzymes are also similar. Importantly, the sequences containing unnatural amino acids at P4-P3 positions were recognized only by both SARS-PLpro, not MERS-PLpro and human UCH-L3. Thus, in the next step we developed covalent inhibitors based on two selected substrate sequences. These inhibitors proved to be active and selectively inhibited of the SARS-PLpro, but much weaker for MERS-PLpro and practically ineffective for human UCH-L3. This is excellent information in terms of conducting research towards the search for peptide antiviral compounds targeted to this enzyme. In our research, we also decided to check whether SARS-CoV-2-PLpro has the ability to bind ubiquitin. Analysis of the enzyme kinetics of the Ub-ACC substrate indicates that it is efficiently processed by the enzyme, but the difference between the tetrapeptide substrate and ubiquitin is only about ten times, when in the case of SARS-CoV-PLpro this difference is around sixty times (Table 1). This indicates some differences between both enzymes in the aspect of interaction in the exosite binding region (Figure 5) related to amino acids identity and similarity. A similar observation also resulted from a study in which we used the Biotin-Ub-VME inhibitor. Both enzymes are effectively inhibited, however SARS-CoV-PLpro with slightly higher efficiency.

In summary, our research shows a very high level of similarity between the two enzymes in terms of substrate specificity near the binding pocket, which can immediately be used to search for effective antiviral molecules, *in silico* drug search as well as retargeting of known drugs. Our data also gives a hope for design of a drug that can act as a pan-selective inhibitor against both SARS-CoV-PLpro and SARS-CoV-2-PLpro, and may have some universal value against emerging coronaviruses in the near future.

Materials and Methods

Plasmids

The cDNA for Papain-Like protease (PLpro) corresponding to aa745-1061 of SARS-CoV-2 NSP3 was codon optimized for *E. coli* expression, synthesized and cloned into pGEX6P-1 (GE Healthcare, UK) using the BamHI and NotI sites by GeneUniversal (USA). The plasmid was transformed into BL21 (DE3) codon plus *E. coli* strain for protein expression.

Protein production, purification and gel-filtration chromatography

SARS-CoV-PLpro, UCH-L3 and MERS-PLpro were obtained as described earlier [14, 25]. The cells were grown in LB broth at 37°C with shaking until the OD600 reached 1.5. 0.1 mM IPTG and 0.1 mM $ZnSO_4$ were added to induce protein expression overnight at 18°C. Cell pellet was resuspended in lysis buffer (20 mM Tris-Cl pH 8.0, 350 mM NaCl and 2 mM β-mercaptoethanol) and lysed using sonication. The lysate was cleared by centrifugation at 35000 g for 30 mins at 4°C. The lysate was passed onto Glutathione Sepharose 4B (GE) followed by washing with lysis buffer. The GST tagged PLpro was eluted in lysis buffer supplemented with 20 mM reduced Glutathione (pH 8.0). The fusion protein was cleaved using GST-PreScission protease at 4°C overnight followed with desalting and passing through fresh glutathione beads to remove cleaved GST and PreScission protease. The sample was further purified using Superdex 200 pg size-exclusion columns (GE) equilibrated with 20 mM Tris-Cl pH 8.0, 40 mM NaCl and 2 mM DTT. The purified protein was then concentrated to ~10 mg/ml and snap frozen in liquid nitrogen for later use.

Reagents

The reagents used for the solid-phase peptide synthesis (SPPS) were as follows: Rink Amide (RA) resin (particle size 100-200 mesh, loading 0.74 mmol/g), 2-chlorotrityl chloride resin (particle size 100-200 mesh, loading 0.97 mmol/g), all Fmoc-amino acids, *O*-benzotriazole-*N*,*N*,*N*`,*N*`-tetramethyl-uronium-hexafluoro-phosphate (HBTU), 2-(1-H-7-azabenzotriazol-1-yl)-1,1,3,3-tetramethyluranium hexafluorophosphate (HATU), piperidine, diisopropylcarbodiimide (DICI) and trifluoroacetic acid (TFA), purchased from Iris Bioteh GmbH (Marktredwitz, Germany); anhydrous *N*-hydroxybenzotriazole (HOBt) from Creosauls Louisville, KY, USA; 2,4,6-collidine (2,4,6-trimethylpyridine), HPLC-grade acetonitrile, triisopropylsilane (TIPS), *t*Bu-N-allyl carbamate, toluene, methyl acrylate, dichlorophenylborane and 2nd generation Grubbs catalyst from Sigma-Aldrich (Poznan, Poland); and *N,N*-diisopropylethylamie (DIPEA) from VWR International (Gdansk, Poland). *N,N*-dimethylformamide (DMF), dichloromethane (DCM), methanol (MeOH), diethyl ether (Et_2O), acetic acid (AcOH), and phosphorus pentoxide (P_2O_5), obtained from Avantor (Gliwice, Poland). Individual substrates, Ub-ACC and B-Ub-VME were purified by HPLC on a Waters M600 solvent delivery module with a Waters M2489 detector system using a semipreparative Wide Pore C8 Discovery column and Jupiter 10 µm C4 300 Å column (250 x 10 mm). The solvent composition was as follows: phase A (water/0.1% TFA) and phase B (acetonitrile/0.1% TFA). The purity of each compound was confirmed with an analytical HPLC system using a

Jupiter 10 µm C4 300 Å column (250 x 4.6 mm). The solvent composition was as follows: phase A (water/0.1% TFA) and phase B (acetonitrile/0.1% TFA); gradient, from 5% B to 95% B over a period of 15 or 20 min. The molecular weight of each substrate and B-Ub-VME was confirmed by high-resolution mass spectrometry on a High-Resolution Mass Spectrometer Waters LCT premier XE with electrospray ionization (ESI) and a time-of-flight (TOF) module.

Combinatorial and defined substrate library synthesis.

Detailed protocol of combinatorial and defined tetrapeptide fluorogenic substrate library synthesis was described elsewhere [26].

Determination of SARS-CoV and SARS-CoV-2-PLpro substrate specificity

Library screening was performed using a spectrofluorometer (Molecular Devices Spectramax Gemini XPS) in 96-well plates containing substrates and enzymes. Assay conditions were 1 µL of substrate in DMSO and 99 µL of enzyme, which had been incubated for 15 min at 37°C in assay buffer (150 mM NaCl, 20 mM Tris, 5 mM DTT, pH 8.0 for SARS-CoV PLpro; 5 mM NaCl, 20 mM Tris, 5 mM DTT, pH 8.0 for SARS-CoV-2 PLpro). The final substrate concentration in each well was 200 µM of combinatorial library and 100 µM of defined P2 library. The final enzyme concentration was 1 µM SARS-CoV-PLpro and 0.5 µM SARS-CoV-2-PLpro for P3 and P4 sublibraries and 0.1 µM SARS-CoV-PLpro and 75 nM SARS-CoV-2-PLpro for Ac-Leu-Arg-P2-Gly-ACC. The release of ACC was measured continuously for 45 min (λ_{ex} = 355 nm, λ_{em} = 460 nm). SARS-CoV and SARS-CoV-2-PLpro substrate specificity profiles were established by setting the highest relative fluorescence unit per second (RFU/s) for the best substrate as to 100% and adjusting other results accordingly.

Synthesis of tetrapeptide fluorogenic substrates and Ub-ACC

Individual fluorogenic substrates were synthesized on a solid support using the SPPS method as previously described [29, 30]. Each substrate was purified by HPLC and analyzed using analytical HPLC and HRMS. The purity of each compound was ≥95%. The individual substrates were dissolved at 20 mM in DMSO and stored at -80°C until use.

Kinetic studies of individual tetrapeptide substrates and Ub-ACC

Individual substrate hydrolysis was measured in the same assay conditions as for library screening. The final substrate concentration was 10 µM, SARS-CoV and SARS-CoV-2-PLpro concentration was 0.1 µM, MERS-CoV PLpro was 2.5 µM, and UCH-L3 was 8.8 µM. MERS-

CoV PLpro and UCH-L3 were incubated for 30 min at 37°C in assay buffer (MERS-CoV PLpro: 150 mM NaCl, 20 mM Tris, 5 mM DTT, pH 8.0; UCH-L3: 50 mM HEPES, 0.5 mM EDTA, 5 mM DTT, pH 7.5) prior to add into the wells on plate. The measurements were repeated at least three times and the results were presented as mean values with standard deviations. Kinetic parameters were determined for selected tetrapeptide substrates and Ub-ACC toward SARS-CoV and SARS-CoV-2 PLpro. Wells contained 20 µL of substrate in assay buffer at eight different concentrations (0.88 µM to 20 µM) and 80 µL of enzyme (0.5 µM SARS-CoV and SARS-CoV-2-PLpro for tetrapeptide substrates and 80 nM SARS-CoV-2-PLpro and 10 nM SARS-CoV-PLpro for Ub-ACC). Substrate hydrolysis was measured for 30 min at the appropriate wavelength (λ_{ex} = 355 nm, λ_{em} = 460 nm). Each experiment was carried out at least three times and the results reported as averages with standard deviation. Due to the precipitation of tetrapeptide substrates at high concentrations, only the specificity constant (k_{cat}/K_M) was determined. When $[S_0] << K_M$, the plot of v_i (the initial velocities) versus $[S_0]$ yields a straight line with slope representing V_{max}/K_M, k_{cat}/K_M = slope/E (E – total enzyme concentration).

SARS-CoV and SARS-CoV-2-PLpro inhibitor and B-Ub-VME synthesis

Inhibitor synthesis was performed in the three sequential stages. In the first step vinyl methyl ester as a reactive group was synthesized according to published protocol [31]. *t*Bu-N-allyl carbamate (500 mg, 3.2 µmol) was dissolved in 10 mL of anhydrous toluene. Methyl acrylate (580 µL, 6.4 µmol), dichlorophenylborane (42 µL, 0.32 µmol) and 2nd generation Grubbs catalyst (50 mg) were added. The reaction was carried out under reflux at 40°C with stirring overnight. After 12 h, the solvent was evaporated under reduce preasure, and the mixture was purified by column chromatography on silica gel (Hex/EtOAc 5:1). The crude product was obtained as a yellowish oil. *t*Bu group deprotection was performed by adding TFA/DCM/TIPS (4.2 mL, 3/1/0.2, *v/v/v*) cleavage mixture for 45 min with stirring. TFA*H_2N-Gly-VME was then crystallized in cold Et_2O and stored at -20°C. In the second step Ac-P4-P3-Gly-OH fragments were synthesized using 2-chlorotrityl chloride resin as previously described [32]. In the last step Ac-P4-P3-Gly-OH fragment (1.2 eq) was coupled to the reactive group (1 eq) using HATU (1.2 eq) and 2,4,6-collidine (3 eq) as a coupling reagents in DMF. The reaction was carried out at RT with stirring for 2h. The reaction mixture was diluted in ethyl acetate, washed once with 5% citric acid, once with 5 % $NaHCO_3$ and once brine, dried over $MgSO_4$, and concentrated under reduce pressure. To remove side chain amino acid protecting groups, Ac-P4-P3-Gly-Gly-VME was added to a mixture of TFA/DCM/TIPS (% v/v/v, 70:27:3). After 30

min, solvents were removed and inhibitor was purified on HPLC. B-Ub-VME was synthesized according to synthetic protocol described elsewhere [33, 34].

Determination of DUB inhibition

To assess activity and selectivity of designed SARS-CoV and SARS-CoV-2-PLpro inhibitors DUBs were incubated with inhibitors at eight different concentrations (2.3 μM to 300 μM) for 30 min at 37°C in assay buffers. DUB residual activity was estimated using Ac-Leu-Arg-Gly-Gly-ACC (50 μM). Assay conditions were 20 μL of inhibitor, 60 μL of DUB (0.3 μM SARS-CoV PLpro, 0.1 μM SARS-CoV-2 PLpro, 2.5 μM MERS-CoV PLpro, and 8 μM UCH-L3), and 20 μL of substrate (50 μM). Inhibition assays were measured for 40 min and repeated at least three times. The results were established as mean values with standard deviations.

SARS-CoV and SARS-CoV-2-PLpro labelling by B-Ub-VME

Enzymes (200 nM) were incubated with different B-Ub-VME concentrations (100, 200, 400, 800, and 1000 nM) in assay buffer (150 mM NaCl, 20 mM Tris, 5 mM DTT, pH 8.0 for SARS-CoV PLpro; 5 mM NaCl, 20 mM Tris, 5 mM DTT, pH 8.0 for SARS-CoV-2 PLpro) for 45 min at 37°C. Then 3x SDS/DTT was added, and the samples were boiled for 5 min at 95°C and resolved on 4-12% Bis-Tris Plus 12-well gels. Electrophoresis was performed at 200 V for 29 min. Next, the proteins were transferred to a nitrocellulose membrane (0.2 μm, Bio-Rad) for 60 min at 10 V. The membrane was blocked with 2% BSA in Tris-buffered saline with 0.1% (v/v) Tween 20 (TBS-T) for 60 min at RT. B-Ub-VME was detected with a fluorescent streptavidin Alexa Fluor 647 conjugate (1:10 000) in TBS-T with 1% BSA using an Azure Biosystems Sapphire Biomolecular Imager and Azure Spot Analysis Software.

Acknowledgments

This project was supported by the National Science Center grant 2015/17/N/ST5/03072 (Preludium 9) in Poland (W.R.) and the "TEAM/2017-4/32" project, which is carried out within the TEAM program of the Foundation for Polish Science, cofinanced by the European Union under the European Regional Development Fund (M.D.). W.R. is a beneficiary of a START scholarship from the Foundation for Polish Science. Research reported in this publication was supported by NIH R01 GM115568 (S.K.O.). Z.L. is a Hollings Cancer Center Postdoctoral Fellow. T.T.H. is supported by NIH grant ES025166. S.J.S is funded by NIH Grant # GM099040-07

Competing interest

The authors declare no competing financial interest.

Author contributions

W.R. S.K.O., and M.D. conceived the project; M. D., W.R. and M.Z. designed the research; W.R., M.Z., and D.N. performed the research and collected data; D.N., Z.L., S.J.S., M.B. and T.T.H. contributed enzymes; M.D., W.R. and M.Z. analyzed and interpreted the data; W.R. and M.D. wrote the manuscript and all authors critically revised the manuscript.

References

1. Zhong, N.S., et al., *Epidemiology and cause of severe acute respiratory syndrome (SARS) in Guangdong, People's Republic of China, in February, 2003.* Lancet, 2003. **362**(9393): p. 1353-1358.
2. de Wit, E., et al., *SARS and MERS: recent insights into emerging coronaviruses.* Nature Reviews Microbiology, 2016. **14**(8): p. 523-534.
3. Zaki, A.M., et al., *Isolation of a Novel Coronavirus from a Man with Pneumonia in Saudi Arabia.* New England Journal of Medicine, 2012. **367**(19): p. 1814-1820.
4. Wang, C., et al., *A novel coronavirus outbreak of global health concern (vol 395, pg 470, 2020).* Lancet, 2020. **395**(10223): p. 496-496.
5. Huang, C., Y. Wang, and X. Li, *Clinical features of patients infected with 2019 novel coronavirus in Wuhan, China (vol 395, pg 497, 2020).* Lancet, 2020. **395**(10223): p. 496-496.
6. Baez-Santos, Y.M., S.E. St John, and A.D. Mesecar, *The SARS-coronavirus papain-like protease: Structure, function and inhibition by designed antiviral compounds.* Antiviral Research, 2015. **115**: p. 21-38.
7. Han, Y.S., et al., *Papain-like protease 2 (PLP2) from severe acute respiratory syndrome coronavirus (SARS-CoV): Expression, purification, characterization, and inhibition.* Biochemistry, 2005. **44**(30): p. 10349-10359.
8. Harcourt, B.H., et al., *Identification of severe acute respiratory syndrome coronavirus replicase products and characterization of papain-like protease activity.* Journal of Virology, 2004. **78**(24): p. 13600-13612.
9. Barretto, N., et al., *The papain-like protease of severe acute respiratory syndrome coronavirus has deubiquitinating activity.* Journal of Virology, 2005. **79**(24): p. 15189-15198.
10. Barretto, N., et al., *Deubiquitinating activity of the SARS-CoV papain-like protease.* Nidoviruses: Toward Control of Sars and Other Nidovirus Diseases, 2006. **581**: p. 37-41.
11. Lindner, H.A., et al., *Selectivity in ISG15 and ubiquitin recognition by the SARS coronavirus papain-like protease.* Archives of Biochemistry and Biophysics, 2007. **466**(1): p. 8-14.
12. Lindner, H.A., et al., *The papain-like protease from the severe acute respiratory syndrome coronavirus is a deubiquitinating enzyme.* Journal of Virology, 2005. **79**(24): p. 15199-15208.
13. Ratia, K., et al., *Structural Basis for the Ubiquitin-Linkage Specificity and deISGylating Activity of SARS-CoV Papain-Like Protease.* Plos Pathogens, 2014. **10**(5).

14. Bekes, M., et al., *SARS hCoV papain-like protease is a unique Lys(48) linkage-specific di-distributive deubiquitinating enzyme.* Biochemical Journal, 2015. **468**: p. 215-226.
15. Bekes, M., et al., *Recognition of Lys48-Linked Di-ubiquitin and Deubiquitinating Activities of the SARS Coronavirus Papain-like Protease.* Molecular Cell, 2016. **62**(4): p. 572-585.
16. Calistri, A., et al., *The Ubiquitin-Conjugating System: Multiple Roles in Viral Replication and Infection.* Cells, 2014. **3**(2): p. 386-417.
17. Mielech, A.M., et al., *MERS-CoV papain-like protease has deISGylating and deubiquitinating activities.* Virology, 2014. **450**: p. 64-70.
18. Devaraj, S.G., et al., *Regulation of IRF-3-dependent innate immunity by the papain-like protease domain of the severe acute respiratory syndrome coronavirus.* Journal of Biological Chemistry, 2007. **282**(44): p. 32208-32221.
19. Clementz, M.A., et al., *Deubiquitinating and Interferon Antagonism Activities of Coronavirus Papain-Like Proteases.* Journal of Virology, 2010. **84**(9): p. 4619-4629.
20. Frieman, M., et al., *Severe Acute Respiratory Syndrome Coronavirus Papain-Like Protease Ubiquitin-Like Domain and Catalytic Domain Regulate Antagonism of IRF3 and NF-kappa B Signaling.* Journal of Virology, 2009. **83**(13): p. 6689-6705.
21. Ratia, K., et al., *A noncovalent class of papain-like protease/deubiquitinase inhibitors blocks SARS virus replication.* Proc Natl Acad Sci U S A, 2008. **105**(42): p. 16119-24.
22. Hilgenfeld, R., *From SARS to MERS: crystallographic studies on coronaviral proteases enable antiviral drug design.* FEBS J, 2014. **281**(18): p. 4085-96.
23. Lin, M.H., et al., *Disulfiram can inhibit MERS and SARS coronavirus papain-like proteases via different modes.* Antiviral Res, 2018. **150**: p. 155-163.
24. Poreba, M., G.S. Salvesen, and M. Drag, *Synthesis of a HyCoSuL peptide substrate library to dissect protease substrate specificity.* Nat Protoc, 2017. **12**(10): p. 2189-2214.
25. Drag, M., et al., *Positional-scanning fluorigenic substrate libraries reveal unexpected specificity determinants of DUBs (deubiquitinating enzymes).* Biochem J, 2008. **415**(3): p. 367-75.
26. Rut, W., et al., *Engineered unnatural ubiquitin for optimal detection of deubiquitinating enzymes.* Biorxiv preprint server, 2020. DOI:https://doi.org/10.1101/2020.01.30.926881.
27. Zhang, L., et al., *Crystal structure of SARS-CoV-2 main protease provides a basis for design of improved alpha-ketoamide inhibitors.* Science, 2020.
28. Jin, Z., et al., *Structure of M(pro) from COVID-19 virus and discovery of its inhibitors.* Nature, 2020.
29. Poreba, M., G.S. Salvesen, and M. Drag, *Synthesis of a HyCoSuL peptide substrate library to dissect protease substrate specificity.* Nature Protocols, 2017. **12**(10): p. 2189-2214.
30. Maly, D.J., et al., *Expedient solid-phase synthesis of fluorogenic protease substrates using the 7-amino-4-carbamoylmethylcoumarin (ACC) fluorophore.* Journal of Organic Chemistry, 2002. **67**(3): p. 910-915.
31. Vedrenne, E., et al., *Dramatic effect of boron-based Lewis acids in cross-metathesis reactions.* Synlett, 2005(4): p. 670-672.
32. Rut, W., et al., *Selective Substrates and Activity-Based Probes for Imaging of the Human Constitutive 20S Proteasome in Cells and Blood Samples.* Journal of Medicinal Chemistry, 2018. **61**(12): p. 5222-5234.
33. El Oualid, F., et al., *Chemical Synthesis of Ubiquitin, Ubiquitin-Based Probes, and Diubiquitin.* Angewandte Chemie-International Edition, 2010. **49**(52): p. 10149-10153.
34. de Jong, A., et al., *Ubiquitin-Based Probes Prepared by Total Synthesis To Profile the Activity of Deubiquitinating Enzymes.* Chembiochem, 2012. **13**(15): p. 2251-2258.